

# Current Biology

## Aspen growth is not limited by starch reserves

### Highlights

- Aspen trees employ a passive starch-storage mechanism during growth
- Carbon assimilation is not limiting growth of aspen trees under benign conditions
- Starch is not required for bud set and bud flush or its timing in aspen trees

### Authors

Wei Wang, Loic Talide, Sonja Viljamaa, Totte Niittyä

### Correspondence

totte.niittyä@slu.se

### In brief

Wang et al. create low-starch aspen mutants and discover that aspen trees employ a passive investing strategy to save carbon for future needs and that tree growth is not carbon limited under benign conditions.



## Report

## Aspen growth is not limited by starch reserves

Wei Wang,<sup>1</sup> Loic Talide,<sup>1</sup> Sonja Viljamaa,<sup>1</sup> and Totte Niittylä<sup>1,2,\*</sup><sup>1</sup>Department of Forest Genetics and Plant Physiology, Swedish University of Agricultural Sciences, Umeå Plant Science Centre, Umeå S-901 83, Sweden<sup>2</sup>Lead contact\*Correspondence: [totte.niittyla@slu.se](mailto:totte.niittyla@slu.se)<https://doi.org/10.1016/j.cub.2022.06.056>

## SUMMARY

All photosynthetic organisms balance CO<sub>2</sub> assimilation with growth and carbon storage. Stored carbon is used for growth at night and when demand exceeds assimilation. Gaining a mechanistic understanding of carbon partitioning between storage and growth in trees is important for biological studies and for estimating the potential of terrestrial photosynthesis to sequester anthropogenic CO<sub>2</sub> emissions.<sup>1,2</sup> Starch represents the main carbon storage in plants.<sup>3,4</sup> To examine the carbon storage mechanism and role of starch during tree growth, we generated and characterized low-starch hybrid aspen (*Populus tremula* × *tremuloides*) trees using CRISPR-Cas9-mediated gene editing of two *PHOSPHOGLUCOMUTASE* (*PGM*) genes coding for plastidial *PGM* isoforms essential for starch biosynthesis. We demonstrate that starch deficiency does not reduce tree growth even in short days, showing that starch is not a critical carbon reserve during diel growth of aspen. The low-starch trees assimilated up to ~30% less CO<sub>2</sub> compared to the wild type under a range of irradiance levels, but this did not reduce growth or wood density. This implies that aspen growth is not limited by carbon assimilation under benign growth conditions. Moreover, the timing of bud set and bud flush in the low-starch trees was not altered, implying that starch reserves are not critical for the seasonal growth-dormancy cycle. The findings are consistent with a passive starch storage mechanism that contrasts with the annual *Arabidopsis* and indicate that the capacity of the aspen to absorb CO<sub>2</sub> is limited by the rate of sink tissue growth.

## RESULTS AND DISCUSSION

Our understanding of how the balance between tree growth and carbon storage is achieved is incomplete and often extrapolated from studies of annual herbs, like *Arabidopsis thaliana*. *Arabidopsis* utilizes an active storage mechanism whereby starch accumulation is adjusted to optimize growth and survival over the entire life cycle.<sup>5</sup> The extent to which the *Arabidopsis*-based model is applicable to trees is unclear. Tree growth models have historically depicted starch reserves as buffers, accumulating excess carbon on a daily or seasonal basis, the so-called passive storage model.<sup>6,7</sup> However, there is also experimental evidence indicating that trees actively store starch at the expense of growth.<sup>7–9</sup>

Multiple studies have indicated a role for starch in providing carbon and energy when photosynthesis or sugar transport is limited, e.g., during dormancy, bud flush, or stress.<sup>8,10–14</sup> A genetic link between seasonal starch content variation and stress has been observed for genomic variation connected to carbon storage in *Populus trichocarpa*. The storage carbohydrate variation in the outer stem and roots during dormancy was heritable and adapted to local climate, with greater starch reserves correlating with warmer and drier environments.<sup>15</sup> The authors observed that genetic variation of stem starch content during dormancy did not correlate with genetic variation in stem diameter, suggesting that storage in the stem is independent of secondary growth in *Populus*.<sup>15</sup> Thus, current results support a role

for starch in stress adaptation and during seasonal changes, but when tree growth is not limited by environmental factors its role remains less clear.<sup>7,8</sup> Leaf starch content of growing almond (*Prunus dulcis*) trees increased during the day and decreased at night, supporting a role for leaf starch in maintaining growth and carbon balance during the diurnal cycle.<sup>16</sup> However, despite many studies documenting tree starch levels, the relationship between starch and tree growth has been difficult to address. Progress has been hampered by the lack of mutant trees with defective starch metabolism. Starch is synthesized from ADP-glucose in the plastids, which in chloroplasts is derived from the reduction of CO<sub>2</sub> in the Calvin cycle.<sup>17</sup> ADP-glucose biosynthesis in the plastids requires the activity of phosphoglucomutase (*PGM*), which facilitates the interconversion of glucose-6-phosphate and glucose-1-phosphate. Glucose-1-phosphate is the substrate of ADP-glucose pyrophosphorylase (*AGPase*), which catalyzes the synthesis of ADP-glucose. Consequently, *Arabidopsis pgm* and *adg1* mutants that lack plastidial *PGM* or *AGPase* contain only limited residual starch.<sup>18–20</sup>

Low-starch aspen *pgm1pgm2* mutants

We identified two plastidial *PHOSPHOGLUCOMUTASE* genes (*PGM1* and *PGM2*) in the *Populus* genome, based on 89% amino acid sequence identity to *Arabidopsis* *PGM1* and the presence of a predicted plastid targeting sequence (Figure S1). CRISPR-Cas9-mediated gene editing was used to create mutations in *PGM1* and *PGM2*. Ten lines containing allelic homozygous



mutations were identified by PCR using gene-specific primers, then restriction enzyme digestion of the PCR products (Figure S1). Two lines—*pgm1pgm2* lines 1 and 2—were selected for detailed characterization. Sequencing the gene-edited loci revealed single base pair insertions causing premature stop codons in the second exon of both *PGM1* and *PGM2* (Figure 1A). Iodine staining indicated that both lines lacked starch in fully expanded source leaves harvested at the end of the light period, and in phloem tissues and root tips (Figures 1B–1D). The low-starch phenotype was confirmed by a quantitative assay, establishing that the double mutants contained no or only trace levels of leaf starch at the end of the photoperiod (Figure 1E).

### Starch is not a critical carbon reserve during diurnal aspen growth

To assess the contribution of starch to tree growth, wild-type (WT) and *pgm1pgm2* trees were grown under 18-h/6-h day/night cycle in an automated phenotyping facility. No significant difference was observed in the height growth rate (Figure 2A) at the end of the growth period, stem thickness, wood density, and biomass of stems and leaves between WT and *pgm1pgm2* lines (Table S1). Root biomass obtained from a separate greenhouse experiment was also similar (Table S1). The only visible difference was a change in the petiole and leaf angle, resulting in slightly drooping leaves (Figure 2B). The leaf angle change caused a reduction in the canopy area of both lines when imaged from above, while in the side view only line 1 differed slightly from the WT (Figures 2C and 2D).

The normal growth of the *pgm1pgm2* trees is reminiscent of the *pgm* mutants of *Lotus japonicus* and *Pisum sativum*, which also grow well under a day/night cycle.<sup>21,22</sup> Thus, the aspen phenotype is not unique in this regard. In contrast, *Arabidopsis* and tobacco *pgm* mutants exhibit carbon depletion at night and significantly reduced growth rates except under very long days or constant light.<sup>20,23</sup> The fully expanded source leaves of WT aspen exhibited clear starch turnover during a diurnal cycle, with higher levels of starch at the end of the day than the end of the night (Figure 3A). These observations suggest that leaf starch supports growth and respiration during the diurnal cycle in aspen but does not play the critical role observed in *Arabidopsis* and tobacco. Investigation of the relationship between day length, growth, and starch levels in trees is complicated by tree species from the temperate zones of the world that have evolved to respond to day-length change to ensure correct timing of growth cessation and dormancy. In the aspen genotype used in this study, shortening of the day to approximately 15 h induces dormancy.<sup>24,25</sup> However, the onset of dormancy takes several weeks and the growth rate is first reduced 3–4 weeks after the change from 18-h/6-h to 14-h/10-h or 8-h/16-h day/night cycle (Figure S2). These results show that the *pgm1pgm2* and WT trees grow at a similar rate under both 14-h/10-h and 8-h/16-h cycles.

### Lack of starch does not affect soluble sugar pools in leaves or developing wood

To further investigate the carbohydrate status of the *pgm1pgm2* trees, we quantified sucrose, glucose, and fructose levels in the youngest fully expanded source leaves of trees grown under an 18-h/6-h day/night cycle. No significant difference between WT

and the mutants was observed (Figure 3B). In contrast, *Arabidopsis* *pgm* mutants accumulate significantly more sucrose, glucose, and fructose during the day compared to WT.<sup>23</sup> We noted that the fully expanded aspen source leaves contained 25–35  $\mu\text{mol g}^{-1} \text{FW}^{-1}$  sucrose, glucose, and fructose, approximately an order of magnitude more than the values reported for *Arabidopsis* rosette leaves.<sup>23,26</sup> The relatively high soluble sugar pool in aspen leaves is thought to be associated with the passive symplasmic phloem loading mechanism.<sup>27,28</sup> In the greenhouse-grown trees, the starch content in fully expanded WT source leaves at the end of the day was, on average, 100–150  $\mu\text{mol glucose equivalents g}^{-1} \text{FW}^{-1}$  (Figures 1 and 3), which is higher but broadly comparable with the 30–60  $\mu\text{mol g}^{-1} \text{FW}^{-1}$  typically reported for *Arabidopsis*.<sup>23,29</sup> The ratio of glucose equivalents in starch and sucrose at the end of the photoperiod in the source leaves between the two different experiments reported in Figures 1 and 3 was similar: 1.7:1 and 1.6:1, respectively. Hence, aspen does not exhibit characteristics of a sucrose-storing species such as barley (*Hordeum vulgare*), which stores more sucrose than starch in leaves.<sup>30</sup> However, the sucrose pool in aspen leaves may be sufficient to maintain sugar homeostasis at night in the low-starch trees. Accordingly, we observed a reduction in the source leaf sucrose content between the end of the day and of the night in both WT and *pgm1pgm2* (Figure 3C). A similar decrease was also observed when comparing source leaves of trees transferred from 18-h/6-h to 8-h/16-h day/night (Figure 3D). To assess whether the source leaves of *pgm1pgm2* trees were experiencing carbon depletion, we analyzed the expression of carbon depletion marker genes at the end of the 16-h night. Quantitative real-time PCR analysis of the *Populus* DARK INDUCIBLE 6 (*DIN6*), DORMANCY-ASSOCIATED PROTEIN-LIKE 1 (*DRM1*), and GIBBERELLIN-STIMULATED ARABIDOPSIS 6 (*GASA6*) gene transcripts previously shown to respond to carbon depletion<sup>31</sup> revealed no significant differences between WT and the mutants (Figure 3E). These results suggest that both starch and sucrose are utilized in aspen at night or when carbon demand exceeds assimilation, but that starch is not critical.

### CO<sub>2</sub> assimilation is reduced in *pgm1pgm2* trees

If carbon was limiting tree growth and/or starch accumulation occurred at the expense of growth, the absence of starch biosynthesis in *pgm1pgm2* could be expected to free more carbon for growth. Since the blocked starch biosynthesis pathway did not cause obvious changes in tree growth, wood density, or soluble sugar levels, we investigated carbon assimilation rates in the WT and mutants. We measured CO<sub>2</sub> assimilation at different light intensities and leaf transpiration as a proxy for stomatal conductance. Under irradiance up to 100  $\mu\text{mol quanta m}^{-2} \text{s}^{-1}$ , the *pgm1pgm2* lines did not differ from WT, but at higher irradiances the mutants showed reduced CO<sub>2</sub> uptake (Figure 4A). No significant difference occurred in leaf transpiration, showing that the reduction in CO<sub>2</sub> assimilation was not caused by reduced stomatal conductance (Figure 4B). To determine whether impaired absorption of light in *pgm1pgm2* source leaves contributed to the reduced CO<sub>2</sub> assimilation rate, we assayed chlorophyll content and the photosynthesis light-dependent reactions. The *pgm1pgm2* leaves had slightly increased chlorophyll content while all of the photosynthetic

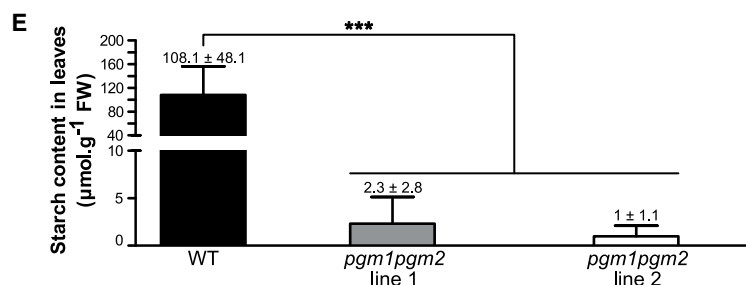
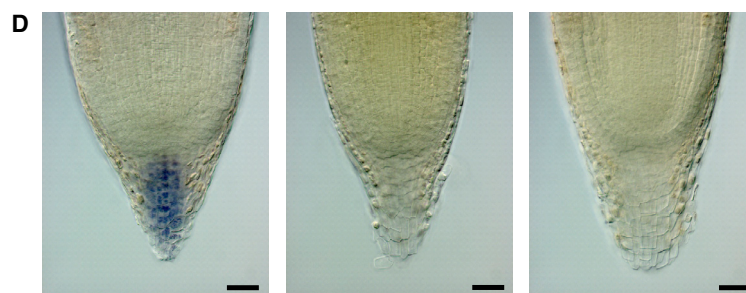
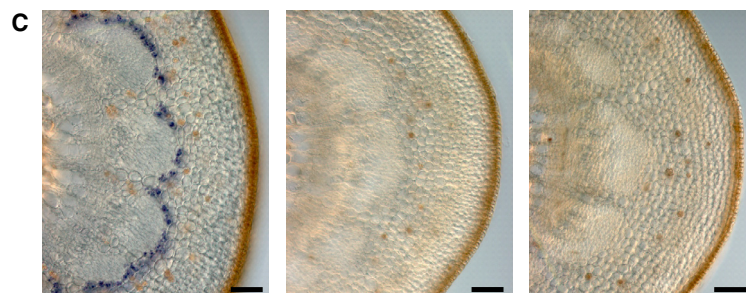
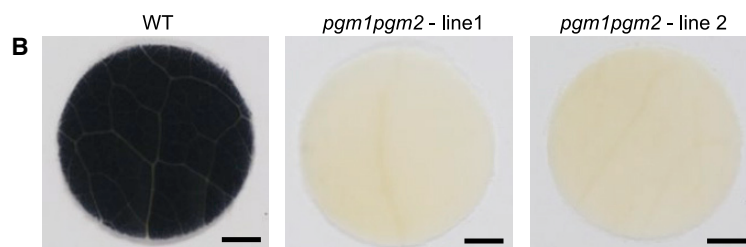
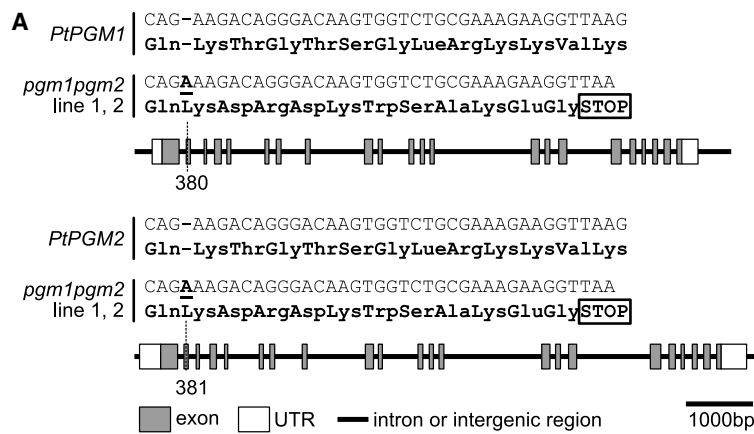


**Figure 1. Mutation of the PHOSPHOGLUCOMUTASE1 and 2 genes in *Populus tremula* × *tremuloides* and the low-starch phenotype of the *pgm1pgm2* mutants**

(A) Schematic diagram showing the gene-edited mutations in the PGM1 and PGM2 genes and the resulting premature stop codons. See also Figure S1.

(B) Iodine-stained leaf discs from fully expanded source leaves of wild-type (WT) and *pgm1pgm2* line 1 and line 2 harvested at the end of the photoperiod.

(C and D) Iodine-stained stem cross-sections (C) and root tips of WT and *pgm1pgm2* line 1 and line 2 (D).

Scale bars, 3 mm (B), 40 μm (C), and 20 μm (D).

(E) Starch content in fully expanded source leaves of WT and *pgm1pgm2* line 1 and line 2. Note discontinuous y axis. Data are mean ± SD from 4, 5, and 5 biological replicates for WT, *pgm1pgm2* line 1, and line 2, respectively. \*\*\*p < 0.001 according to one-way ANOVA and Tukey post hoc test. See also Figure S4.

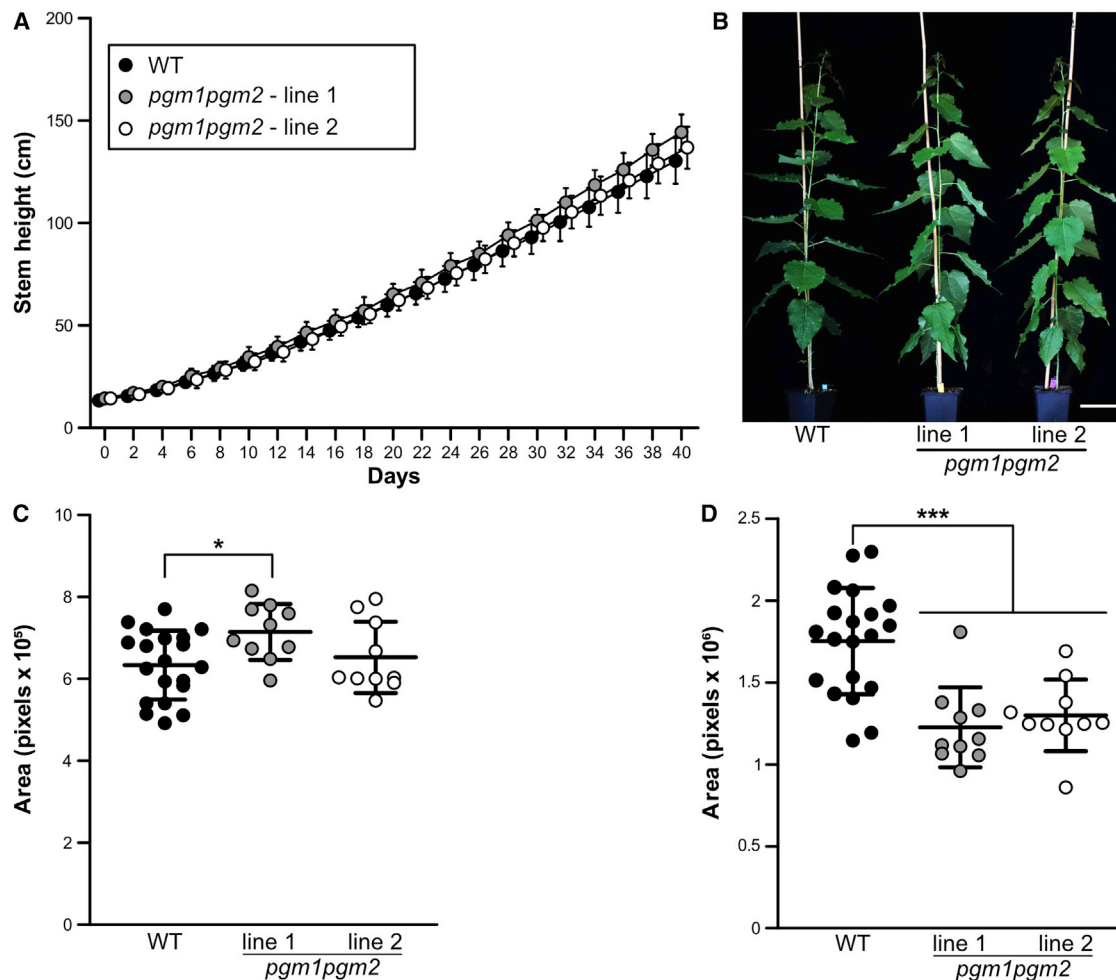


**Figure 2. Morphology of *Populus tremula* × *tremuloides* WT and *pgm1pgm2* mutant trees**

(A) Height growth rate of trees grown in an automated phenotyping facility for 40 days in an 18-h photoperiod.

(B) Morphology of 1-month-old trees grown in an 18-h photoperiod. Scale bar, 10 cm.

(C and D) Canopy area imaged from the side (C) and from above (D).

Data are mean ± SD from 20, 10, and 10 biological replicates for WT, *pgm1pgm2* line 1, and line 2, respectively. \*\*\**p* < 0.001 and \*\**p* < 0.05 according to one-way ANOVA and Tukey post hoc test.

See also [Figures S2](#) and [S3](#) and [Table S1](#).

parameters were comparable between the mutants and WT ([Table S2](#)). We conclude that impaired absorption of light in *pgm1pgm2* leaves does not explain the reduced CO<sub>2</sub> assimilation rate; a more likely explanation is a reduced flux through the photosynthetic carbon reduction cycle.

### Control of carbon flux to starch in aspen leaves differs from Arabidopsis

In the automated growth phenotyping experiments, the photosynthetically active light intensity was 180–200 μmol quanta m<sup>-2</sup> s<sup>-1</sup>. It was possible that, at this level, the difference in the CO<sub>2</sub> assimilation rate between *pgm1pgm2* and WT is still too subtle to affect growth. To test this, the trees were grown under 500 μmol quanta m<sup>-2</sup> s<sup>-1</sup> for 8 weeks. The mutants and WT again exhibited similar growth rate and wood density ([Figure S2](#)) while the CO<sub>2</sub> assimilation rate, but not stomatal conductance, was still reduced in the *pgm1pgm2* trees ([Figures 4C](#) and [4D](#)).

Reduced photosynthesis in response to increasing light intensity has also been observed in the *pgm* and *adg* Arabidopsis mutants.<sup>20,32</sup> However, one difference is that the photosynthesis is light saturated earlier in Arabidopsis *pgm* mutants compared to WT.<sup>32</sup> In the *pgm1pgm2* and WT aspen leaves, the rate of CO<sub>2</sub> assimilation in response to increasing light begins to deviate after 100 μmol quanta m<sup>-2</sup> s<sup>-1</sup> for both genotypes and does not become saturated until >1,500 ([Figure 4](#)).

We hypothesized that the lack of inhibition of CO<sub>2</sub> assimilation at ≤ 100 μmol quanta m<sup>-2</sup> s<sup>-1</sup> in *pgm1pgm2* aspens may reflect low carbon flux to the starch biosynthesis pathway in low light, and consequently lack of feedback inhibition of CO<sub>2</sub> assimilation when the pathway is blocked in the *pgm1pgm2*. To explore this, we compared the source leaf starch levels in WT trees grown in 18-h/6-h day/night cycles under irradiance of ~150 and ~70 μmol quanta m<sup>-2</sup> s<sup>-1</sup>. Even under the lower irradiance the trees continued to grow, suggesting growth adaptation to low

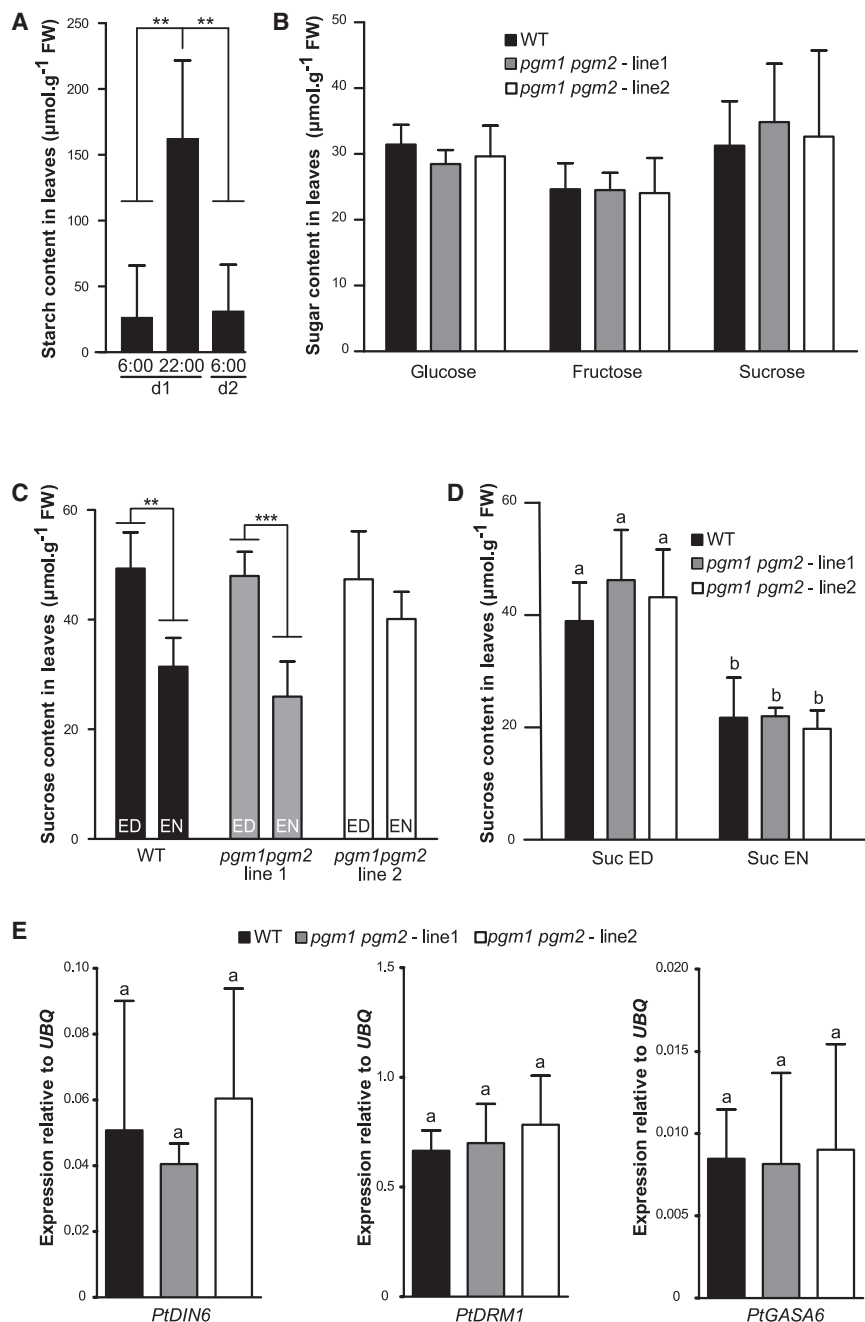


**Figure 3. Starch, soluble sugar content, and carbon depletion marker gene expression in *Populus tremula* × *tremuloides* WT and *pgm1pgm2* leaves**

(A) WT source leaf starch content at the onset of the photoperiod day 1 (06:00-d1), at the end of the photoperiod day 1 (22:00-d1), and at the onset of the photoperiod day 2 (06:00-d2). Data are mean  $\pm$  SD from 5 biological replicates.

(B) Glucose, fructose, and sucrose levels in leaves from WT and *pgm1pgm2* grown in 18-h photoperiod in the middle of the photoperiod. Data are mean  $\pm$  SD from 4, 5, and 5 biological replicates for WT, *pgm1pgm2* line 1, and line 2, respectively.

(C) Source leaf sucrose content in WT and *pgm1pgm2* mutant trees grown in 18-h photoperiod. Samples were harvested at the end of day (ED) and at the end of night (EN). Data are mean  $\pm$  SD from 5 biological replicates.

(A–C) \*\*\* $p < 0.001$  and \*\* $p < 0.01$  according to one-way ANOVA and Tukey post hoc test.

(D) Sucrose content in the source leaves of WT and *pgm1pgm2* trees after 10 days under 8-h short-day conditions. ED, end of the day; EN, end of the night.

(E) Relative transcript expression levels of carbon depletion genes in source leaves of WT and *pgm1pgm2* harvested at the end of the night after 10 days under 8-h short-day conditions. *PtUBQ* is used as a reference.

(D and E) Values are means  $\pm$  SD,  $n = 5$  biological replicates.  $p < 0.05$  according to one-way ANOVA and Tukey post hoc test. FW, fresh weight.

See also Figure S2.

light and carbon supply (Figure S2). The trees growing in under  $\sim 70 \mu\text{mol quanta m}^{-2} \text{s}^{-1}$  contained only  $\sim 10 \mu\text{mol g}^{-1} \text{FW}^{-1}$  starch at the end of the day while the trees under  $\sim 150 \mu\text{mol quanta m}^{-2} \text{s}^{-1}$  contained  $\sim 74 \mu\text{mol g}^{-1} \text{FW}^{-1}$  (Figure S2) and  $100\text{--}160 \mu\text{mol g}^{-1} \text{FW}^{-1}$  in the experiments with variable greenhouse light conditions of  $150\text{--}200 \mu\text{mol quanta m}^{-2} \text{s}^{-1}$  (Figures 1E and 3A). Thus, irradiance level correlates positively with source leaf starch content in aspen, and under limiting light, the rate of starch synthesis is drastically reduced while growth is proportionally less affected. There is also a correlation between leaf starch and irradiance levels in Arabidopsis.<sup>29</sup> However, the fact that Arabidopsis *pgm* mutants exhibit severe growth

defects<sup>20</sup> while the *pgm1pgm2* trees grow well shows that the control mechanism of carbon flux to leaf starch and its importance for growth differs between these species.

**Wood composition is not altered in the *pgm1pgm2* trees**

Carbon partitioning and whole-tree carbon balance are known to influence wood composition in aspen.<sup>33,34</sup> Hence, wood was analyzed by pyrolysis-GC/MS, providing a comprehensive wood composition fingerprint by detecting 200–300 pyrolytic degradation products.<sup>35</sup> This analysis established that wood carbohydrate and lignin content, as well as carbohydrate:lignin ratio, did not differ significantly between WT and the *pgm1pgm2* lines (Figure S3). Neither did the evaluation of the entire MS spectra using principal component analysis reveal differences between WT and the mutants (Figure S3), further confirming that starch is not critical during aspen growth.

**Bud set and bud flush are not altered in *pgm1pgm2* trees**

Starch reserves in the roots, stem, and branches vary during the year in trees. In deciduous trees at the beginning of the growing

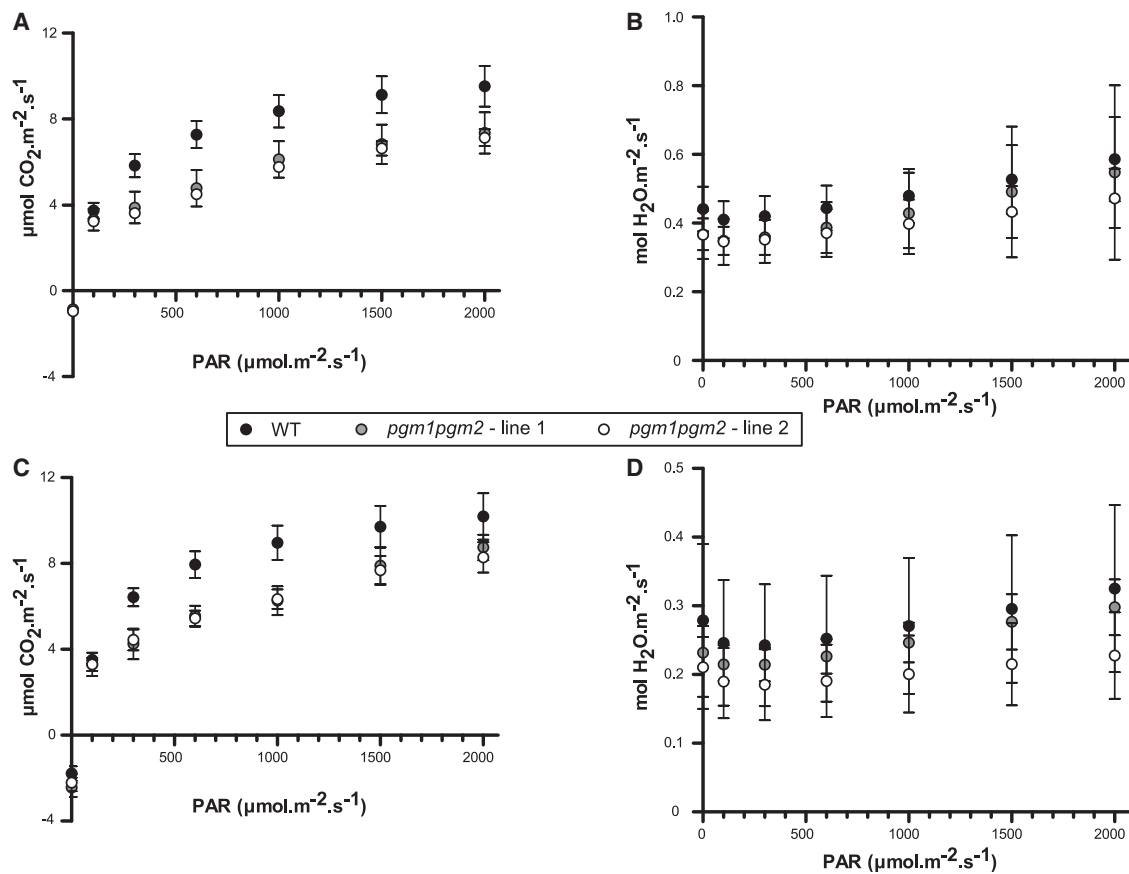


**Figure 4. Effect of light intensity on the rate of CO<sub>2</sub> assimilation and stomatal conductance in the source leaves of *Populus tremula* × *tremuloides* WT and *pgm1pgm2* mutant trees**

(A and B) CO<sub>2</sub> assimilation rate (A) and stomatal conductance (B) in source leaves of trees grown under 180–200 μmol quanta m<sup>-2</sup> s<sup>-1</sup>. (C and D) CO<sub>2</sub> assimilation rate (C) and stomatal conductance (D) of source leaves in trees grown under 500 μmol quanta m<sup>-2</sup> s<sup>-1</sup>. Photosynthetically active radiation (PAR). Data are mean ± SD from 4 biological replicates.

See also Table S2.

season, starch reserves appear to be mobilized for the formation of new leaves.<sup>36–38</sup> To examine the role of starch in this process, we compared the timing of bud flush in *pgm1pgm2* and WT trees. The trees were grown under 18-h light period for 6 weeks and then 14-h light period for 10 weeks to induce growth cessation, bud set, and dormancy. No difference between *pgm1pgm2* and WT trees was observed during the dormancy process (Figure S4). After dormancy induction the trees were exposed to 10 weeks of cold (4°C) followed by an 18-h light period at 22°C/18°C light/dark to induce bud flush. The bud flush process was monitored daily, but no difference between *pgm1pgm2* and WT trees was observed (Figure S4). These results confirm that starch synthesis is not required for dormancy onset and bud flush in aspen. The bud set and bud flush results combined with the lack of strong tree growth defects in the *pgm1pgm2* under different day lengths point to a passive starch storage mechanism, implying that aspen does not actively direct carbon to starch to ensure carbon supply for future growth and development.

Our observation that CO<sub>2</sub> assimilation was reduced in *pgm1pgm2* without obvious effects on the rate of tree

growth and biomass accumulation indicates that carbon availability does not limit tree growth. Growth was also probably not limited by water or mineral nutrients since trees were regularly watered and fertilized. This suggests processes downstream of CO<sub>2</sub> assimilation as limiting for tree growth under benign growing conditions. Accordingly, several ecophysiological studies of tree growth under diverse natural conditions have suggested that sink activity controlled by the environment and developmental cues restricts trees' capacity to assimilate to atmospheric CO<sub>2</sub>.<sup>39,40</sup> In conclusion, we suggest that aspen passively accumulates starch reserves that support growth and survival over a tree's lifespan. To elucidate the long-term consequences of low starch and reduced CO<sub>2</sub> assimilation, a comparison of whole-tree carbon budgets over multiple growth-dormancy cycles is needed. These are key issues when developing models of terrestrial carbon dynamics, building on understanding physiological processes underlying carbon dynamics in trees; indeed, there is both genetic and physiological evidence for the role of starch under adverse growth conditions and changing climate.<sup>8,10,15</sup>

## STAR★METHODS

Detailed methods are provided in the online version of this paper and include the following:

- **KEY RESOURCES TABLE**
- **RESOURCE AVAILABILITY**
  - Lead contact
  - Materials availability
- **EXPERIMENTAL MODEL AND SUBJECT DETAILS**
  - Plant material and growth conditions
- **METHOD DETAILS**
  - *PGM1PGM2* CRISPR vector construction, hybrid aspen transformation and genotyping
  - Phylogenetic analysis
  - Lugol staining
  - Sugar and starch measurement
  - RNA quantification and qPCR
  - Wood density measurement
  - Wood composition analysis using pyrolysis-GC/MS
  - Photosynthetic parameters
  - Bud set and bud break scoring
  - Bacteria species and strains
  - Accession numbers
- **QUANTIFICATION AND STATISTICAL ANALYSIS**
  - Statistical analysis
  - Data and code availability

## SUPPLEMENTAL INFORMATION

Supplemental information can be found online at <https://doi.org/10.1016/j.cub.2022.06.056>.

## ACKNOWLEDGMENTS

We thank Junko Takahashi-Schmidt and the UPSC Biopolymer Analytical Platform for help with the wood analysis and Edward Carlsson for help with starch measurements. This work was supported by the Swedish Research Council for Sustainable Development (Formas) (project grant 2016-01322), Bio4Energy (Swedish Programme for Renewable Energy), and the UPSC Centre for Forest Biotechnology funded by VINNOVA.

## AUTHOR CONTRIBUTIONS

W.W., S.V., and L.T. conducted the experiments; W.W., S.V., L.T., and T.N. designed the experiments; and T.N. conceived the study and wrote the paper with contributions from all authors.

## DECLARATION OF INTERESTS

The authors declare no competing interests.

Received: February 8, 2022

Revised: April 13, 2022

Accepted: June 16, 2022

Published: July 11, 2022

## REFERENCES

1. Bastin, J.F., Finegold, Y., Garcia, C., Mollicone, D., Rezende, M., Routh, D., Zohner, C.M., and Crowther, T.W. (2019). The global tree restoration potential. *Science* 365, 76–79. <https://doi.org/10.1126/science.aax0848>.
2. IPCC (2018). Intergovernmental Panel on Climate Change (IPCC), An IPCC Special Report on the Impacts of Global Warming of 1.5°C Above Pre-Industrial Levels. <https://www.ipcc.ch/sr15/download/#chapter>.
3. Stitt, M., and Zeeman, S.C. (2012). Starch turnover: pathways, regulation and role in growth. *Curr. Opin. Plant Biol.* 15, 282–292. <https://doi.org/10.1016/j.pbi.2012.03.016>.
4. Kozłowski, T.T. (1992). Carbohydrate sources and sinks in woody plants. *Bot. Rev.* 58, 107–222. <https://doi.org/10.1007/bf02858600>.
5. Smith, A.M., and Stitt, M. (2007). Coordination of carbon supply and plant growth. *Plant Cell Environ.* 30, 1126–1149. <https://doi.org/10.1111/j.1365-3040.2007.01708.x>.
6. Le Roux, X., Lacombe, A., Escobar-Gutierrez, A., and Le Dizes, S. (2001). Carbon-based models of individual tree growth: a critical appraisal. *Ann. For. Science* 58, 469–506. <https://doi.org/10.1051/forest:2001140>.
7. Sala, A., Woodruff, D.R., and Meinzer, F.C. (2012). Carbon dynamics in trees: feast or famine? *Tree Physiol.* 32, 764–775. <https://doi.org/10.1093/treephys/tpr143>.
8. Dietze, M.C., Sala, A., Carbone, M.S., Czimczik, C.I., Mantooth, J.A., Richardson, A.D., and Vargas, R. (2014). Nonstructural carbon in woody plants. *Annu. Rev. Plant Biol.* 65, 667–687. <https://doi.org/10.1146/annurev-arplant-050213-040054>.
9. Huang, J., Hammerbacher, A., Gershenzon, J., van Dam, N.M., Sala, A., McDowell, N.G., Chowdhury, S., Gleixner, G., Trumbore, S., and Hartmann, H. (2021). Storage of carbon reserves in spruce trees is prioritized over growth in the face of carbon limitation. *Proc. Natl. Acad. Sci. USA* 118, e2023297118, <https://doi.org/10.1073/pnas.2023297118>.
10. Klein, T., and Hoch, G. (2015). Tree carbon allocation dynamics determined using a carbon mass balance approach. *New Phytol.* 205, 147–159. <https://doi.org/10.1111/nph.12993>.
11. Essiamah, S., and Eschrich, W. (1985). Changes of starch content in the storage tissues of deciduous trees during winter and spring. *IAWA Bulletin* 6, 97–106. <https://doi.org/10.1163/22941932-90000921>.
12. Sauter, J.J., and van Cleve, B. (1994). Storage, mobilization and interrelations of starch, sugars, protein and fat in the ray storage tissue of poplar trees. *Trees (Berl.)* 8, 297–304. <https://doi.org/10.1007/bf00202674>.
13. Noronha, H., Silva, A., Dai, Z., Gallusci, P., Rombolà, A.D., Delrot, S., and Gerós, H. (2018). A molecular perspective on starch metabolism in woody tissues. *Planta* 248, 559–568. <https://doi.org/10.1007/s00425-018-2954-2>.
14. Berrocal-Lobo, M., Ibañez, C., Acebo, P., Ramos, A., Perez-Solis, E., Collada, C., Casado, R., Aragoncillo, C., and Allona, I. (2011). Identification of a homolog of *Arabidopsis* DSP4 (SEX4) in chestnut: its induction and accumulation in stem amyloplasts during winter or in response to the cold. *Plant Cell Environ.* 34, 1693–1704. <https://doi.org/10.1111/j.1365-3040.2011.02365.x>.
15. Blumstein, M., Richardson, A., Weston, D., Zhang, J., Muchero, W., and Hopkins, R. (2020). A new perspective on ecological prediction reveals limits to climate adaptation in a temperate tree species. *Curr. Biol.* 30, 1447–1453.e4. <https://doi.org/10.1016/j.cub.2020.02.001>.
16. Tixier, A., Orozco, J., Roxas, A.A., Earles, J.M., and Zwieniecki, M.A. (2018). Diurnal variation in nonstructural carbohydrate storage in trees: remobilization and vertical mixing. *Plant Physiol.* 178, 1602–1613. <https://doi.org/10.1104/pp.18.00923>.
17. Smith, A.M., and Zeeman, S.C. (2020). Starch: a flexible, adaptable carbon store coupled to plant growth. *Annu. Rev. Plant Biol.* 71, 217–245. <https://doi.org/10.1146/annurev-arplant-050718-100241>.
18. Lin, T.-P., Caspar, T., Somerville, C., and Preiss, J. (1988). Isolation and characterization of a starchless mutant of *Arabidopsis thaliana* (L.) Heynh lacking ADPglucose pyrophosphorylase activity. *Plant Physiol.* 86, 1131–1135. <https://doi.org/10.1104/pp.86.4.1131>.
19. Lin, T.-P., Caspar, T., Somerville, C.R., and Preiss, J. (1988). A starch deficient mutant of *Arabidopsis thaliana* with low ADPglucose

- pyrophosphorylase activity lacks one of the two subunits of the enzyme. *Plant Physiol.* 88, 1175–1181. <https://doi.org/10.1104/pp.88.4.1175>.
20. Caspar, T., Huber, S.C., and Somerville, C. (1985). Alterations in growth, photosynthesis, and respiration in a starchless mutant of *Arabidopsis thaliana* (L.) deficient in chloroplast phosphoglucomutase activity. *Plant Physiol.* 79, 11–17. <https://doi.org/10.1104/pp.79.1.11>.
  21. Harrison, C.J., Hedley, C., and Wang, T.L. (1998). Evidence that the *rug3* locus of pea (*Pisum sativum* L.) encodes plastidial phosphoglucomutase confirms that the imported substrate for starch synthesis in pea amyloplasts is glucose-6-phosphate. *Plant J.* 13, 753–762.
  22. Vriet, C., Welham, T., Brachmann, A., Pike, M., Pike, J., Perry, J., Parniske, M., Sato, S., Tabata, S., Smith, A.M., and Wang, T.L. (2010). A suite of *Lotus japonicus* starch mutants reveals both conserved and novel features of starch metabolism. *Plant Physiol.* 154, 643–655. <https://doi.org/10.1104/pp.110.161844>.
  23. Gibon, Y., Blasing, O.E., Palacios-Rojas, N., Pankovic, D., Hendriks, J.H.M., Fisahn, J., Hohne, M., Gunther, M., and Stitt, M. (2004). Adjustment of diurnal starch turnover to short days: depletion of sugar during the night leads to a temporary inhibition of carbohydrate utilization, accumulation of sugars and post-translational activation of ADP-glucose pyrophosphorylase in the following light period. *Plant J.* 39, 847–862. <https://doi.org/10.1111/j.1365-313X.2004.02173.x>.
  24. Nilsson, O., Aldén, T., Sitbon, F., Little, C.H.A., Chalupa, V., Sandberg, G., and Olsson, O. (1992). Spatial pattern of cauliflower mosaic virus 35S promoter luciferase expression in transgenic hybrid aspen trees monitored by enzymatic assay and non-destructive imaging. *Transgenic Res.* 1, 209–220. <https://doi.org/10.1007/bf02524751>.
  25. Olsen, J.E., Junttila, O., Nilsen, J., Eriksson, M.E., Martinussen, I., Olsson, O., Sandberg, G., and Moritz, T. (1997). Ectopic expression of oat phytochrome A in hybrid aspen changes critical daylength for growth and prevents cold acclimatization. *Plant J.* 12, 1339–1350. <https://doi.org/10.1046/j.1365-313x.1997.12061339.x>.
  26. Blasing, O.E., Gibon, Y., Gunther, M., Hohne, M., Morcuende, R., Osuna, D., Thimm, O., Usadel, B., Scheible, W.R., and Stitt, M. (2005). Sugars and circadian regulation make major contributions to the global regulation of diurnal gene expression in *Arabidopsis*. *Plant Cell* 17, 3257–3281. <https://doi.org/10.1105/tpc.105.035261>.
  27. Rennie, E.A., and Turgeon, R. (2009). A comprehensive picture of phloem loading strategies. *Proc. Natl. Acad. Sci. USA* 106, 14162–14167. <https://doi.org/10.1073/pnas.0902279106>.
  28. Turgeon, R., and Medville, R. (1998). The absence of phloem loading in willow leaves. *Proc. Natl. Acad. Sci. USA* 95, 12055–12060. <https://doi.org/10.1073/pnas.95.20.12055>.
  29. Moraes, T.A., Mengin, V., Annunziata, M.G., Encke, B., Krohn, N., Höhne, M., and Stitt, M. (2019). Response of the circadian clock and diel starch turnover to one day of low light or low CO<sub>2</sub>. *Plant Physiol.* 179, 1457–1478. <https://doi.org/10.1104/pp.18.01418>.
  30. Sicher, R.C., Kremer, D.F., and Harris, W.G. (1984). Diurnal carbohydrate metabolism of barley primary leaves. *Plant Physiol.* 76, 165–169. <https://doi.org/10.1104/pp.76.1.165>.
  31. Tarancón, C., González-Grandío, E., Oliveros, J.C., Nicolas, M., and Cubas, P. (2017). A conserved carbon starvation response underlies bud dormancy in woody and herbaceous species. *Front. Plant Sci.* 8, 788. <https://doi.org/10.3389/fpls.2017.00788>.
  32. Ekkehard Neuhaus, H., and Stitt, M. (1990). Control analysis of photosynthate partitioning: impact of reduced activity of ADP-glucose pyrophosphorylase or plastid phosphoglucomutase on the fluxes to starch and sucrose in *Arabidopsis thaliana* (L.). *Heynh. Planta* 182, 445–454. <https://doi.org/10.1007/bf02411398>.
  33. Dominguez, P.G., Donev, E., Derba-Maceluch, M., Bünder, A., Hedenström, M., Tomášková, I., Mellerowicz, E.J., and Niittylä, T. (2021). Sucrose synthase determines carbon allocation in developing wood and alters carbon flow at the whole tree level in aspen. *New Phytol.* 229, 186–198. <https://doi.org/10.1111/nph.16721>.
  34. Gerber, L., Zhang, B., Roach, M., Rende, U., Gorzsás, A., Kumar, M., Burgert, I., Niittylä, T., and Sundberg, B. (2014). Deficient sucrose synthase activity in developing wood does not specifically affect cellulose biosynthesis, but causes an overall decrease in cell wall polymers. *New Phytol.* 203, 1220–1230. <https://doi.org/10.1111/nph.12888>.
  35. Gerber, L., Eliasson, M., Trygg, J., Moritz, T., and Sundberg, B. (2012). Multivariate curve resolution provides a high-throughput data processing pipeline for pyrolysis-gas chromatography/mass spectrometry. *J. Anal. Appl. Pyrol.* 95, 95–100. <https://doi.org/10.1016/j.jaap.2012.01.011>.
  36. Gough, C.M., Flower, C.E., Vogel, C.S., and Curtis, P.S. (2010). Phenological and temperature controls on the temporal non-structural carbohydrate dynamics of *Populus grandidentata* and *Quercus rubra*. *Forests* 1, 65–81. <https://doi.org/10.3390/f1010065>.
  37. Landhäusser, S.M., and Lieffers, V.J. (2003). Seasonal changes in carbohydrate reserves in mature northern *Populus tremuloides* clones. *Trees Struct. Funct.* 17, 471–476. <https://doi.org/10.1007/s00468-003-0263-1>.
  38. Regier, N., Streb, S., Zeeman, S.C., and Frey, B. (2010). Seasonal changes in starch and sugar content of poplar (*Populus deltoides* x *nigra* cv. Dorskamp) and the impact of stem girdling on carbohydrate allocation to roots. *Tree Physiol.* 30, 979–987. <https://doi.org/10.1093/treephys/tpq047>.
  39. Körner, C. (2003). Carbon limitation in trees. *J. Ecol.* 91, 4–17. <https://doi.org/10.1046/j.1365-2745.2003.00742.x>.
  40. Körner, C. (2015). Paradigm shift in plant growth control. *Curr. Opin. Plant Biol.* 25, 107–114. <https://doi.org/10.1016/j.pbi.2015.05.003>.
  41. Koncz, C., and Schell, J. (1986). The promoter of TL-DNA gene 5 controls the tissue-specific expression of chimaeric genes carried by a novel type of *Agrobacterium* binary vector. *Mol. Gen. Genet.* 204, 383–396. <https://doi.org/10.1007/bf00331014>.
  42. Xing, H.-L., Dong, L., Wang, Z.-P., Zhang, H.-Y., Han, C.-Y., Liu, B., Wang, X.-C., and Chen, Q.-J. (2014). A CRISPR/Cas9 toolkit for multiplex genome editing in plants. *BMC Plant Biol.* 14, 327. <https://doi.org/10.1186/s12870-014-0327-y>.
  43. Kumar, S., Stecher, G., and Tamura, K. (2016). MEGA7: molecular evolutionary genetics analysis version 7.0 for bigger datasets. *Mol. Biol. Evol.* 33, 1870–1874. <https://doi.org/10.1093/molbev/msw054>.
  44. Fahlgren, N., Feldman, M., Gehan, M.A., Wilson, M.S., Shyu, C., Bryant, D.W., Hill, S.T., McEntee, C.J., Warnasoorya, S.N., Kumar, I., et al. (2015). A versatile phenotyping system and analytics platform reveals diverse temporal responses to water availability in *Setaria*. *Mol. Plant* 8, 1520–1535. <https://doi.org/10.1016/j.molp.2015.06.005>.
  45. Schneider, C.A., Rasband, W.S., and Eliceiri, K.W. (2012). NIH Image to ImageJ: 25 years of image analysis. *Nat. Methods* 9, 671–675. <https://doi.org/10.1038/nmeth.2089>.
  46. Roach, M., Gerber, L., Sandquist, D., Gorzsás, A., Hedenström, M., Kumar, M., Steinhäuser, M.C., Feil, R., Daniel, G., Stitt, M., et al. (2012). Fructokinase is required for carbon partitioning to cellulose in aspen wood. *Plant J.* 70, 967–977. <https://doi.org/10.1111/j.1365-313x.2012.04929.x>.
  47. Hendriks, J.H., Kolbe, A., Gibon, Y., Stitt, M., and Geigenberger, P. (2003). ADP-glucose pyrophosphorylase is activated by posttranslational redox-modification in response to light and to sugars in leaves of *Arabidopsis* and other plant species. *Plant Physiol.* 133, 838–849. <https://doi.org/10.1104/pp.103.024513>.
  48. Smith, A.M., and Zeeman, S.C. (2006). Quantification of starch in plant tissues. *Nat. Protoc.* 1, 1342–1345. <https://doi.org/10.1038/nprot.2006.232>.
  49. Xu, M., Zang, B., Yao, H.S., and Huang, M.R. (2009). Isolation of high quality RNA and molecular manipulations with various tissues of *Populus*. *Russ. J. Plant Physiol.* 56, 716–719. <https://doi.org/10.1134/s1021443709050197>.
  50. Livak, K.J., and Schmittgen, T.D. (2001). Analysis of relative gene expression data using real-time quantitative PCR and the 2<sup>-ΔΔCT</sup> method. *Methods* 25, 402–408. <https://doi.org/10.1006/meth.2001.1262>.

51. Fataftah, N., Bag, P., André, D., Lihavainen, J., Zhang, B., Ingvarsson, P.K., Nilsson, O., and Jansson, S. (2021). GIGANTEA influences leaf senescence in trees in two different ways. *Plant Physiol.* *187*, 2435–2450. <https://doi.org/10.1093/plphys/kiab439>.
52. Rohde, A., Storme, V., Jorge, V., Gaudet, M., Vitacolonna, N., Fabbrini, F., Ruttink, T., Zaina, G., Marron, N., Dillen, S., et al. (2011). Bud set in poplar - genetic dissection of a complex trait in natural and hybrid populations. *New Phytol.* *189*, 106–121. <https://doi.org/10.1111/j.1469-8137.2010.03469.x>.
53. Ibañez, C., Kozarewa, I., Johansson, M., Ogren, E., Rohde, A., and Eriksson, M.E. (2010). Circadian clock components regulate entry and affect exit of seasonal dormancy as well as winter hardiness in *Populus* trees. *Plant Physiol.* *153*, 1823–1833. <https://doi.org/10.1104/pp.110.158220>.

## STAR★METHODS

### KEY RESOURCES TABLE

REAGENT or RESOURCE	SOURCE	IDENTIFIER
<b>Bacterial and virus strains</b>		
<i>Escherichia coli</i> OmniMAX 2	ThermoFisher Scientific	Cat. No. C854003
<i>Agrobacterium tumefaciens</i> GV3101	<sup>41</sup>	N/A
<b>Chemicals, peptides, and recombinant proteins</b>		
RNeasy Mini Kit	Qiagen	Cat. No. 74106
Maxima First Strand cDNA Synthesis Kit	ThermoFisher Scientific	Cat. No. K1672
iQ SYBR Green Supermix	Bio-Rad	Cat. No. 1708880
Lugol solution	Sigma	Cat. No. L6146
$\alpha$ -Amylase	Roche	Cat. No. 10102814001
$\alpha$ -Amyloglucosidase	Roche	Cat. No. 10102857001
Hexokinase	Roche	Cat. No. 11426362001
Glucose-6-Phosphate Dehydrogenase	Roche	Cat. No. 10737232001
Phosphoglucose Isomerase	Roche	Cat. No. 10128139001
Invertase	Sigma	Cat. No. I4504-5G
Phusion High-Fidelity DNA Polymerase	ThermoFisher Scientific	Cat. No. F530S
FastDigest Eco311	ThermoFisher Scientific	Cat. No. FD0293
T4 DNA Ligase	ThermoFisher Scientific	Cat. No. 15224041
<b>Experimental models: Organisms/strains</b>		
Poplar: <i>Populus tremula</i> x <i>tremuloides</i> T89	N/A	N/A
Poplar: <i>pgm1pgm2</i> – line1	This study	N/A
Poplar: <i>pgm1pgm2</i> – line2	This study	N/A
<b>Oligonucleotides</b>		
PtPGM1-CR-F: CGCTTAGCTCTTCTCTTTCTGT	This study	N/A
PtPGM1-CR-R: TTCTCAGCATCCAACATCCAG	This study	N/A
PtPGM2-CR-F: TTAGTTCTTCCCTCTCTGTCA	This study	N/A
PtPGM2-CR-R: CTACTTTCTCAGCAACCAACAG	This study	N/A
PtDIN6-F: TGTTATCGCCCATCTGTACGAG	This study	N/A
PtDIN6-R: GATGAAATCCACACGGACCCATC	This study	N/A
PtDRM1-F: CCTCTTAACATCAAAGATATTGAC	This study	N/A
PtDRM1-R: GCAAGGTTGCTACCAGGGTGG	This study	N/A
PtGASA6-F: GTTGCTGTCTTCTCTTGGCTC	This study	N/A
PtGASA6-R: CACCTCCTCGTGCATTGTGATG	This study	N/A
PtUBQ-F: GTTGATTTTGTGGGAAGC	This study	N/A
PtUBQ-R: GATCTTGGCCTTACGTTGT	This study	N/A
<b>Recombinant DNA</b>		
Plasmid: pHSE401	<sup>42</sup>	Addgene Plasmid # 62201
Plasmid: pCBC-DT1T2	<sup>42</sup>	Addgene Plasmid # 50590
Plasmid: pHSE401-PGM1PGM2	This study	N/A
<b>Software and algorithms</b>		
GraphPad Prism	GraphPad Software	<a href="https://www.graphpad.com/scientific-software/prism/">https://www.graphpad.com/scientific-software/prism/</a>
Affinity Designer	Serif (Europe)	<a href="https://affinity.serif.com/en-us/designer/">https://affinity.serif.com/en-us/designer/</a>
MEGA7	<sup>43</sup>	<a href="https://www.megasoftware.net/">https://www.megasoftware.net/</a>

(Continued on next page)

**Continued**

REAGENT or RESOURCE	SOURCE	IDENTIFIER
SIMCA 16	Sartorius AG	<a href="https://www.sartorius.com/en/products/process-analytical-technology/data-analytics-software/mvda-software/simca">https://www.sartorius.com/en/products/process-analytical-technology/data-analytics-software/mvda-software/simca</a>
PlantCV	Donald Danforth Plant Science Center <sup>44</sup>	<a href="https://plantcv.readthedocs.io/en/stable/">https://plantcv.readthedocs.io/en/stable/</a>
ImageJ	<sup>45</sup>	<a href="https://imagej.nih.gov/ij/">https://imagej.nih.gov/ij/</a>

**RESOURCE AVAILABILITY**

**Lead contact**

Further information and requests for resources and reagents should be directed to and will be fulfilled by the lead contact, Totte Niittylä ([totte.niittyla@slu.se](mailto:totte.niittyla@slu.se)).

**Materials availability**

All unique/stable reagents generated in this study are available from the [Lead Contact](#) with a completed Materials Transfer Agreement.

**Data and code availability**

- All data reported in this paper will be shared by the [lead contact](#) upon request.
- This paper does not report original code.
- Any additional information required to reanalyze the data reported in this paper is available from the [lead contact](#) upon request.

**EXPERIMENTAL MODEL AND SUBJECT DETAILS**

*Populus tremula x tremuloides* clone T89 was used as the experimental model.

**Plant material and growth conditions**

Hybrid aspens (*Populus tremula x tremuloides*) were micropropagated from cuttings, grown *in vitro* for four weeks as described in Nilsson et al.<sup>24</sup> and then transferred to soil. The trees were grown in the greenhouse, controlled growth rooms or an automated phenotyping facility in a commercial soil/sand/fertilizer mixture (Yrkes Plantjord; Weibulls Horto, <http://www.weibullshorto.se>). In the greenhouse and growth rooms the trees were fertilized using approximately 200 ml of 1% Rika-S (N/P/K 7:1:5; Weibulls Horto) once a week after 3 weeks of planting. The temperature was at 20/18 °C (light/dark).

In the automated phenotyping platform experiment two *pgm1pgm2* mutant lines (10 replicate trees per line) and WT (20 replicate trees) were grown in an equal volume of commercial soil (K-jord; Hasselforsgarden), watered two times a day, fertilized every 2 days with 50 ml 0.6% Rika-S (Weibulls Horto) and treated with Nemasys C on week 4 and 7 after potting. Photoperiod was 18-h light / 6-h dark, and temperature 22°C / 18°C light/dark and relative humidity 60%. Light irradiance was between 150-200  $\mu\text{mol m}^{-2} \text{s}^{-1}$ . The experiment was performed in the tree phenotyping platform (WIWAM Conveyor, SMO, Eeklo, Belgium) described in <https://www.upsc.se/plant-growth-facilities-at-upsc-and-slu-umea/325-upsc-tree-phenotyping-platform.html>. In the facility the trees move on a WIWAM Conveyor belt (SMO, Eeklo, Belgium) and pass every day through an automated watering and weighing station followed by a light curtain which measures tree height. After the height measurement the trees are photographed by three Imperx B4820 RGB-cameras from the side, from above and a focus on the lower part of the stem. The images and the height measurement data in .csv format are recorded on the WIWAM computer and visualized using the PIPPA web interface (<https://pippa.psb.ugent.be/>). Stem widths were measured from the focused stem images using ImageJ.<sup>45</sup> Tree canopy area was determined from the pictures taken from the side and from above using the RGB image workflow of the PlantCV software.<sup>44</sup> After 8 weeks the trees were harvested, and the total fresh weight of stem and leaves including petioles determined using an analytical balance (Sartorius Entris BCE32021-1S, precision 0.01 g). The root biomass of WT and *pgm1pgm2* mutants was measured in a separate greenhouse experiment (18-h/6-h light/dark) after roots were carefully separated from soil.

**METHOD DETAILS**

**PGM1PGM2 CRISPR vector construction, hybrid aspen transformation and genotyping**

*pgm1pgm2* mutants were generated by gene editing of the *PGM1* and *PGM2* genes in the *Populus tremula x tremuloides* T89 background by using CRISPR-Cas9 and a pair of guide RNAs (gRNAs) targeting both *PGM1* and *PGM2*: GCTGAACCTGAAGGCATCA

and CAATTGAGGGTCAGAAGAC. The CRISPR–Cas9 and gRNA sequences were cloned into the pHSE401 vector as described in Xing et al.<sup>42</sup> The construct was introduced into trees by *Agrobacterium*-mediated plant transformation of stem segments as described in Nilsson et al.<sup>24</sup> Independent transgenic lines were screened by PCR and restriction enzyme digestion to identify lines that were homozygous for gene-edited mutant alleles of both *PGM1* and *PGM2* (Figure S1). Mutations in the *PGM1* gene were identified by PCR using primers PtPGM1-CR-F: CGCTTAGCTCTTCTCTTTCTGT and PtPGM1-CR-R: TTCTCAGCATCCAAACATCCAG and digested with Bpil (Thermo Fisher Scientific). Mutations in the *PGM2* gene were identified by PCR using primers PtPGM2-CR-F: TTAGTTCTTCCCTCTGTCA and PtPGM2-CR-R: CTACTTCTCAGCAACCAAACAG and digested with Bpil (Thermo Fisher Scientific).

### Phylogenetic analysis

The phylogenetic analysis was performed by Maximum Likelihood method in MEGA7.<sup>43</sup> The evolutionary history was deduced by the JTT matrix-based model. The tree with the highest log likelihood was selected. The initial tree for the heuristic search was obtained by applying BioNJ algorithms and Neighbor-Join to a matrix of pairwise distances with a JTT model and the topology with superior log likelihood value. The phylogenetic tree was drawn to scale and the branch lengths were measured in the number of substitutions per site. The analysis utilised seven PGM amino acid sequences from *Arabidopsis thaliana* and *Populus trichocarpa*.

### Lugol staining

Leaf discs were harvested and incubated in fixation solution containing 80% ethanol (v/v), 5% formic acid (v/v) and 15% H<sub>2</sub>O (v/v) at 80 °C for 10 min. The fixation solution was then replaced with 80% ethanol (v/v) and samples were incubated at 80 °C for 5 min. Ethanol was removed and leaf discs were stained in Lugol solution (Sigma, L6146) at room temperature for 3 min. Lugol solution was removed by rinsing leaf discs with distilled H<sub>2</sub>O and incubated in fresh H<sub>2</sub>O at 80 °C for 15 min and then at 4 °C for 15 min. For root tips and stem sections, WT and *pgm1pgm2* samples were incubated in 80% ethanol (v/v) for 10 min and then submerged in Lugol solution for 1 min. The samples were rinsed twice with distilled water and then mounted onto microscopy slides using clearing solution (80 g chloralhydrate, 30 mL glycerol and 10 mL water) as the mounting medium. The roots and stem sections were visualized with a Zeiss Axioplan 2 microscope equipped with differential interference contrast optics.

### Sugar and starch measurement

Glucose, fructose and sucrose were extracted and measured as previously described in Roach et al.<sup>46</sup> The ethanol extraction pellet was used as starting material for starch determination, which was performed combining methods described by Hendriks et al.<sup>47</sup> and Smith and Zeeman.<sup>48</sup> Starch was gelatinized by resuspending the pellet into 0.1 M NaOH and incubating at 95 °C for 30 min, after which the samples were acidified by adding a mixture of 0.1 M sodium acetate/NaOH (pH 4.9) and 0.5 M HCl. Three technical replicates were prepared, and 50 mM sodium acetate/NaOH buffer,  $\alpha$ -amylase and  $\alpha$ -amylglucosidase was added to each of the sub-samples for starch degradation. Starch derived glucose was released by three overnight digestions at +37 °C under rotation, removing the supernatant for later analysis and adding new starch digestions mix each day. The amount of released glucose was quantified using an enzymatic assay as described in Roach et al.<sup>46</sup>

### RNA quantification and qPCR

WT and *pgm1pgm2* trees were first grown for 4 weeks in 18-h/6-h day/night cycle and then transferred to an 8-h/16-h day/night cycle for 10 days. Total RNA was extracted from the top most fully expanded source leaf using the CTAB–LiCl method.<sup>49</sup> RNA concentration was determined by NanoDrop 2000 (ThermoFisher Scientific). 1  $\mu$ g of total RNA from each sample was used for cDNA synthesis using the Maxima First Strand cDNA Synthesis Kit (ThermoFisher Scientific) according to the manufacturer's instructions. Quantitative real-time PCR was performed with a Bio-Rad CFX384 Touch Real-Time PCR Detection System, and the numerical values of transcript levels obtained using the relative quantification method.<sup>50</sup> 20  $\mu$ L of 1x iQ SYBR Green Supermix (Bio-Rad) was used for the reaction and the final concentration of each primer was 250 nM. Primers were designed with GC content between 40 to 60% and melting temperature between 50 and 60 °C. The specificity of the primers was checked by BLAST against the *Populus tremula x tremuloides* T89 genome sequence at <https://plantgenie.org>. The amplification specificity of each primer pair was verified by a melting curve (55 °C to 95 °C) exhibiting a single peak. The transcript levels of the carbon depletion genes were normalized to the expression level of *POLYUBIQUITIN 4 (PtUBQ)*.<sup>51</sup> The primer sequences were: PtDIN6-F: TGTTATCGCCCATCTGTACGAG and PtDIN6-R: GATGAAATCCACACGGACCCATC. PtDRM1-F: CCTCTTAACATCAAAGATATTGAC and PtDRM1-R: GCAAGGTTGC TACCAGGTGG. PtGASA6-F: GTTGCTGTCTTCTCTTGGCTC and PtGASA6-R: CACCTCCTCGTGCATTGTGATG. PtUBQ-F: GTTGATTTTTGCTGGGAAGC and PtUBQ-R: GATCTTGGCCTTACGTTGT.

### Wood density measurement

A 2 cm stem segment harvested 10 cm above the soil was used for wood density analysis. Wood density was measured on a dry weight per wet volume basis. Wood pieces were placed in water on an XA105 analytical balance with precision of 0.01 mg (Mettler Toledo; <https://www.mt.com/>) and submerged to determine the sample volume based on displaced water weight. Samples were then oven dried at 102 °C for 24 h and weighed again to obtain the dry mass weight. The wood density was calculated from the dry weight-to-wet volume ratio.

### Wood composition analysis using pyrolysis-GC/MS

Stems from automated phenotyping facility grown trees were debarked and the developing wood removed by scraping. The stem samples were freeze-dried for 72-h, and then filed to fine wood powder. 60  $\mu\text{g}$  aliquots of the wood powder were weighed using a high-precision microbalance (Mettler Toledo XP6), with three technical replicates of each biological sample. These samples were applied to a pyrolyzer equipped with an auto sampler (PY-2020iD and AS-1020E, Frontier Lab, Japan) connected to a GC/MS (7890A/5975C; Agilent Technologies AB, Sweden). The pyrolysate was separated and analyzed according to the method described by Gerber et al.<sup>35</sup> Data analysis by principal component analysis was performed using the SIMCA 16 software (version 16.0.1.7928, Umetrics AB, Sweden).

### Photosynthetic parameters

Light-response curve of photosynthesis rate and  $\text{H}_2\text{O}$  gas exchange rates were measured for top most fully expanded source leaf at mid-day at different photon irradiances (0, 50, 100, 300, 700, 1200, 1500 and 1800  $\text{mmol s}^{-1} \text{m}^{-2}$ ) using Licor portable gas exchange system (LI-COR 6400XT, <http://www.licor.com>). Leaf pigment and photosynthetic parameters were measured using a SPEEDZEN 200 (JBEAMBio) imaging system as described in Fataftah et al.<sup>51</sup> The leaves for the pigment and photosynthetic parameter determination were detached from the tree at mid-day and equilibrated in the dark prior to the measurements. The nonphotochemical chlorophyll fluorescence quenching (NPQ) was determined as in Fataftah et al.<sup>51</sup> using 1800  $\mu\text{mol}$  actinic light for 3.5 min with 5400  $\mu\text{mol}$  saturating pulses at 30 sec intervals.

### Bud set and bud break scoring

WT and *pgm1pgm2* trees were grown under 18-h/6-h day/night cycle for 6 weeks and then transferred to 14-h/10-h day/night cycle for 10 weeks. Height, number of leaves formed after initiation of SD treatment and bud set stages were scored weekly as described previously.<sup>52</sup> Dormant trees were then placed in a cold room at 4 °C for 10 weeks and then bud break was induced by transferring the trees to normal long day conditions (18-h/6-h light/dark, 21 °C). Bud-break stages of the apical buds were scored daily.<sup>53</sup>

### Bacteria species and strains

*Escherichia coli* OmniMAX 2 strain (ThermoFisher Scientific, Waltham, Massachusetts, United States) was used for CRISPR-Cas9 construct cloning and *Agrobacterium tumefaciens* strain GV3101 was used for aspen transformation.

### Accession numbers

Sequence data from this article can be found in Phytozome *Populus trichocarpa* genome sequence version 10.1 or TAIR website under the following numbers: PtPGM1: POTRI.015G134700. PtPGM2: POTRI.012G132500. PtPGM3: POTRI.010G109500. PtPGM4: POTRI.008G132500. AtPGM: AT5G51820. AtPGM2: AT1G70730. AtPGM3: AT1G23190. PtDIN6: POTRI.009G072900. PtDRM1: POTRI.004G047100. PtGASA6: POTRI.017G083000. PtUBQ: POTRI.001G418500.

## QUANTIFICATION AND STATISTICAL ANALYSIS

### Statistical analysis

For multiple data sets comparisons, one-way ANOVA and Tukey post hoc test was performed. p values < 0.05 were considered as statistically significant differences.

### Data and code availability

GraphPad Prism software was used for statistical analyses and graph construction. Affinity Designer software was used to prepare the figures and tables. MEGA7 software<sup>43</sup> was used for the phylogenetic analysis. SIMCA 16 software was used for principal component analysis. ImageJ software<sup>45</sup> was used to measure the stem width. The PlantCV software<sup>44</sup> was used to determine the tree canopy area.